Ref.TH.2062-CERN

ABSORPTION EFFECTS IN ELASTIC AND INELASTIC DIFFRACTION *)

K. Fiałkowski +) and H.I. Miettinen ++)
CERN - Geneva

A B S T R A C T

We review some recent progress in the analysis of the absorption structure of diffractive processes. The unitarity bound of Pumplin and its various phenomenological consequences are studied. We show that elastic and inelastic diffractions are closely interdependent and strongly influence each other. Consequently, they should not be treated separately but be analyzed together. We discuss how such an analysis may be carried out and to what extent the results may change the present picture of diffraction scattering and hadron structure. We find, among other things, that the proton matter distribution may well be drastically different from that suggested by the analysis of Chou and Yang. Finally, we speculate about how diffractive processes will approach asymptopia.

Invited paper presented at the VIth International
Colloquium on Multiparticle Reactions
Oxford — 14-19 July 1975

---

*) Presented by K. Fiałkowski.

+) On leave from the Jagellonian University, Cracow, Poland.

++) Herman Rosenberg Foundation Fellow. On leave from the Research Institute for Theoretical Physics, University of Helsinki, Finland.

Address after 15 August 1975 : SLAC, Stanford, CA. 94305, U.S.A.

Ref.TH.2062-CERN
12 August 1975

1. INTRODUCTION

Recently, significant progress has been achieved in the analysis of the s channel structure of diffractive processes. In particular, it has become clear that elastic and inelastic diffractive processes are closely interdependent and should not be treated separately. This contradicts the past practice and belief that elastic scattering may be analyzed either by completely ignoring the inelastic diffractive channels or by treating their effects as a small correction, and vice versa. The new developments suggest that many of the problems concerning both elastic and inelastic diffraction should be reanalyzed and that, in many cases, new results may be obtained.

In this talk we shall summarize the results of two recent papers [1),2)] on the relationship between the elastic and the inelastic diffractive processes and, in particular, on the constraints which s channel unitarity imposes on the b space profiles of the diffractive amplitudes.

The plan of the talk is the following. We first recall the assumptions and sketch a simple derivation of the unitarity bound of Pumplin [3)]. We then summarize the results of Ref. 1) concerning the phenomenological relevance of this bound (Section 3). In particular, the necessity of the peripheral character of inelastic diffraction in proton-proton collisions will be shown. In Sections 4 to 6, the results of Ref. 2) are summarized. We first analyze the physical picture that underlies the Pumplin bound (Section 4). We derive a simple formula that illustrates very well the physics underlying the bound, namely, the regeneration nature of diffraction dissociation. We also discuss the experimental estimates for the diffractive cross-sections and study their implications. Section 5 is devoted to a discussion of the multi-channel eikonal approach. We point out, among other things, that the proton matter distribution may well be drastically different from that suggested by the Chou-Yang analysis. In Section 6, we speculate about the asymptotic picture of hadron collisions. Finally, a few conclusions are drawn.

In the following, the phenomenological discussion will be restricted to proton-proton scattering for which the best data exist.

2. PUMPLIN'S BOUND

Let us begin by briefly sketching the derivation of the Pumplin bound.

Assume that there is an unspecified - but finite - number of diffractive states produced. We label them by $|1\rangle,\ldots,|N\rangle$, $|1\rangle$ being the elastic state. Non-diffractive states will be labelled by $|N+1\rangle,\ldots$. Introducing the notation

$$S = 1 + iT = 1 - t \qquad (1)$$

we can write the t matrix in the basis of states defined above. This representation defines a $N\times N$ sub-matrix whose elements are the transition amplitudes among the physical diffractive states. In the following, we shall restrict our discussion to this sub-matrix. Since no confusion can arise, we shall denote it by t, too.

The next step is to diagonalize this diffractive t matrix. We assume it to be real, for simplicity (this corresponds to neglecting the real parts of the diffractive amplitudes). Time-reversal invariance implies that it is symmetric. As is well known, a real symmetric matrix is diagonalized by a unitary transformation. Such a transformation corresponds to a rotation in the space considered which, in the present case, is the sub-space of the diffractive states. The physical diffractive states and the diffractive "eigenstates" (which, by definition, do not undergo inelastic diffractive transitions) are related by

$$|i\rangle = \sum_{k=1}^{N} U_{ik}\,|\Psi_k\rangle \qquad i = 1,\ldots N \qquad (2)$$

Here, $\{|i\rangle, i=1,\ldots,N\}$ and $\{|\Psi_k\rangle, k=1,\ldots,N\}$ are the physical basis and the diffractive eigenbasis, respectively. The coefficients U_{ik} are the elements of the unitary matrix that diagonalizes t.

In the following, we shall work in the impact parameter representation. It follows from angular momentum conservation that all the following formulae are valid for each impact parameter separately.

Since the eigenvalues of the t matrix (the "eigenamplitudes") are normalized linear combinations of real and bounded amplitudes (those describing the scattering of the physical states), they are obviously real and bounded, too :

$$0 \leqslant \lambda_n \leqslant 1 \qquad n = 1,\ldots N \qquad (3)$$

Our normalization is such that $\lambda_n = 1$ corresponds to total absorption of the n^{th} eigenstate.

The total, elastic and inelastic diffractive cross-sections

$$\left[\sigma_i \equiv \sigma_i(s,b) \equiv \frac{1}{2\pi} \frac{d\sigma_i}{db^2} \quad , \quad i = tot, \ el \ , \ diff \right]$$

may be expressed in terms of the t matrix elements as follows :

$$\begin{aligned} \sigma_{tot} &= t_{11} \\ \sigma_{el} &= \frac{1}{2} (t_{11})^2 \\ \sigma_{diff} &= \frac{1}{2} \sum_{k=2}^{N} (t_{1k})^2 \end{aligned} \tag{4}$$

Using the eigenvalue representation

$$\begin{aligned} t_{11} &= \sum_{k=1}^{N} |U_{1k}|^2 \lambda_k \\ (t^2)_{11} &= \sum_{k=1}^{N} |U_{1k}|^2 \lambda_k^2 \end{aligned} \tag{5}$$

we easily obtain the bound

$$\boxed{\sigma_{el}(s,b) + \sigma_{diff}(s,b) \leq \frac{1}{2} \sigma_{tot}(s,b)} \quad \left\{ \begin{matrix} \text{Pumplin's} \\ \text{bound} \end{matrix} \right\} \tag{6}$$

If the total and elastic cross-sections are known, Eq. (6) provides an upper bound for the diffractive inelastic cross-section

$$\sigma_{diff}(s,b) \leq \frac{1}{2} \sigma_{tot}(s,b) - \sigma_{el}(s,b) \tag{7}$$

3. APPLICATION OF THE PUMPLIN BOUND

In Ref. 1), the bound Eq. (7) was applied to high energy proton-proton scattering. The main results of this work may be summarized as follows :

a) Integrating the bound Eq. (7), one obtains an upper bound for the total inelastic diffractive cross-section

$$\sigma_{diff} \leq \frac{1}{2}\sigma_{tot} - \sigma_{el}$$

The numerical value for the right-hand side of this equation at top ISR energy (1500 GeV/c) is about 13 mb. At lower energies, it is slightly less (e.g., 12 mb at 100 GeV/c). The experimental estimates for σ_{diff} (which will be discussed in more detail in Section 4) vary between 6 and 9 mb. Thus the integrated bound is not saturated.

b) A more detailed study of the relevance of the differential bound Eq. (7) was carried out. Inserting in this equation the values of $\sigma_{tot}(b)$ and $\sigma_{el}(b)$ taken from an impact parameter analysis of ISR elastic scattering data [4], the bound shown in Fig. 1 was obtained. Although the result a) implies that the differential bound is not saturated at all impact parameters, this bound is so restrictive at small b that an integrated value of $\sigma_{diff} \approx 7$ mb can be obtained only if $\sigma_{diff}(b)$ is much more peripheral than $\sigma_{el}(b)$.

Many phenomenological analyses of proton-proton diffraction dissociation data had previously suggested that the impact parameter distribution $\sigma_{diff}(b)$ would be peripheral [5]. The results of Ref. 1) provided a direct proof that this is so and, also, clarified to some extent the physical mechanism that is causing this peripherality.

Before continuing the discussion, a word of warning is needed. Although the experimental estimates using very different definitions of "diffractive scattering" agree on the size of σ_{diff} within the large errors quoted above, it is not obvious that all this cross-section is of absorptive nature. Even less is known about the absorptive character of the eigenamplitudes. However, it seems unlikely that any corrections due to non-absorptive contributions (such as non-vanishing real parts of the amplitudes) would change the <u>qualitative</u> features of our results.

4. <u>PROBABILISTIC INTERPRETATION</u>

The formulae of Section 2 may be given a simple interpretation. First, let us note that the total cross-section is given by the average value of the eigenamplitudes weighted by their respective couplings to the two-proton state

$$\sigma_{tot}(b) \equiv t_{11}(b) = \sum_{k=1}^{N} |U_{1k}|^2 \langle \psi_k | t | \psi_k \rangle \equiv \sum_{k=1}^{N} P_k t_k \equiv \langle t_k(b) \rangle \; ; \; t_k \equiv \lambda_k \tag{8}$$

The corresponding formula for the inelastic diffractive cross-section is

$$\boxed{\sigma_{diff}(b) = \tfrac{1}{2}\left(\langle t_k^2(b) \rangle - \langle t_k(b) \rangle^2 \right) \equiv \tfrac{1}{2} D^2(b)} \tag{9}$$

Thus, we see that the total inelastic diffractive cross-section is given by the dispersion squared of the spectrum of the eigenamplitudes that couple to the two-proton state. Equations (8) and (9) are illustrated in Fig. 2.

Our result, Eq. (9), is obviously a generalization of the classical Good-Walker picture of diffraction dissociation [6]. In the Good-Walker approach, the inelastic diffractive processes were treated as regeneration processes and their strengths were proportional to the differences of the absorption strengths of the "bare particle" states. This idea is expressed mathematically in a very clear way by Eq. (9). In particular, we see from this equation that if all the diffractive eigenstates (the "bare particle states" in the Good-Walker language) were absorbed equally strongly, so that the eigenamplitude spectrum were a delta-peak, there would be no inelastic diffraction. A special example of such an extreme case is that of the elastic amplitude saturating the black disc limit.

We also see from Eq. (9) that a large cross-section for inelastic diffraction necessarily implies large variations in the opacities of the strongly coupling eigenamplitudes, and vice versa. It is then natural to ask : what does the experimental size of σ_{diff} imply for the eigenamplitude spectrum ? In particular, should the observed amount of inelastic diffraction be regarded as small or large ? As we shall demonstrate, the answer to these very interesting questions is that the observed size of σ_{diff} in proton-proton scattering should be regarded as extremely large, since it implies that the eigenamplitude spectrum is not only very broad but even double-peaked : the two-proton state couples most strongly either to very black or to very transparent eigenstates.

Let us first summarize the experimental estimates of the ratio of the inelastic diffractive to the elastic cross-section [7]. They are compiled in Fig. 3. Also shown is an estimate resulting from a triple Regge fit to data [8]. Although the various estimates vary considerably and are even to some extent mutually inconsistent (this is mainly due to the different definitions of σ_{diff} used by different authors), one may safely conclude that σ_{diff} is of the same order as σ_{el}, i.e., between 6 and 9 mb at the FNAL-ISR energy range.

In order to see what the above value of σ_{diff} implies for the eigenamplitude spectrum, we proceeded as follows. Using the mean value $\langle t_k(b)\rangle = t_{11}(b)$ taken from the elastic scattering analysis of Ref. 4) and shown in Fig. 1, we calculated for each b the diffractive cross-section $\sigma_{diff}(b)$ resulting from various assumed spectra of eigenamplitudes. The corresponding total diffractive cross-section σ_{diff} was then obtained by integrating $\sigma_{diff}(b)$ over b. A collection of results is shown in Fig. 4. Intuitively, we expected the eigenamplitude spectrum to peak around its mean value (i.e., to be something like a Gaussian). From the results of Fig. 4 we see, however, that such a spectrum corresponds to a diffractive cross-section which is by an order of magnitude too small compared to the experimental value ! We have studied a large set of parametrizations for the eigenamplitude spectrum and may summarize our findings as follows : the experimental size of σ_{diff} implies that at least for the impact parameters that contribute most of σ_{diff} (b=0.5-1 fm), the eigenamplitude distribution must be double-peaked, i.e., the two-proton state must consist mainly either of almost black ($t_k \approx 1$) or of very transparent ($t_k \approx 0$) eigenstates. This result dramatically contradicts the idea suggested by many authors [9] that the physical two-proton state would be very near a diffractive eigenstate and that, consequently, perturbative methods would be particularly applicable to the study of diffraction dissociation.

Next, let us note that the distribution that saturates the Pumplin bound is a bi-delta distribution in which all the contributing eigenamplitudes are either completely black or completely transparent. As we have seen above, the proton-proton eigenamplitude distribution should be qualitatively similar to such a distribution. This illustrates well our point that inelastic diffraction is experimentally nearly as large as unitarity allows.

A convenient way to describe the eigenamplitude spectrum is to express the eigenamplitudes t_k in terms of "eigeneikonals", Ω_k,

$$t_k(b) = 1 - e^{-\Omega_k(b)}$$

and to parametrize the eigeneikonal spectrum $d\sigma/d\Omega_k$. A smoothly varying eigeneikonal spectrum may well generate a double peaked t_k spectrum :

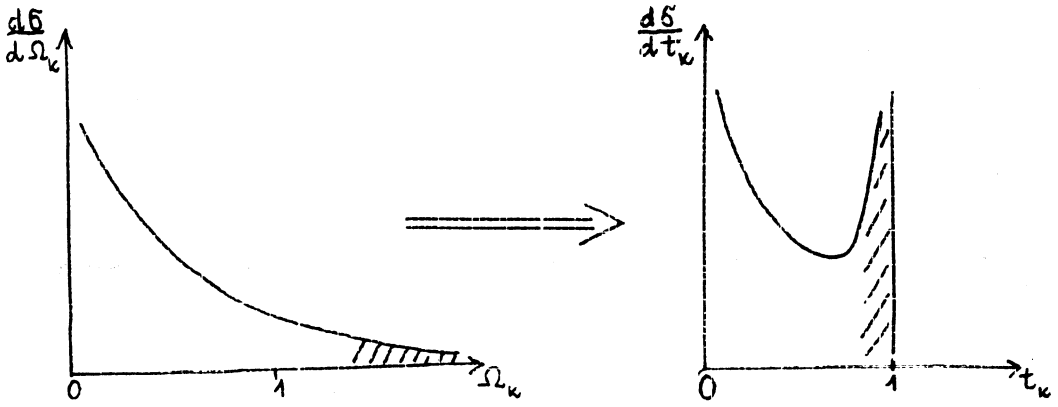

This is easy to see. For small values of Ω_k, the amplitude and the eikonal are approximately equal,

$$t_k = \Omega_k - \frac{1}{2!}\Omega_k^2 + \ldots\ldots \approx \Omega_k$$

and, consequently, the two spectra are nearly equal. A double peaked t_k spectrum may be obtained if the Ω_k spectrum has a "tail" at large Ω_k's, since the eikonalization procedure will map such a tail into a peak near $t_k = 1$, as illustrated above.

We conclude this discussion of the properties of the eigenamplitude spectrum by commenting on the physical interpretation of the above results. After we learnt from experiment that the proton-proton eigenamplitude spectrum must be very broad, we have given much thought to the following questions : what is the physical interpretation of the eigenstates ? Why is the eigenamplitude spectrum so broad ? And, in particular, what do our results teach us about the internal structure of the proton ? Good and Walker interpreted the diffractive eigenstates as eigenstates of the "bare particle" number operator. We do not fully understand this interpretation. Why should a state of a fixed number of "bare particles" (partons, gluons, quarks ?) not undergo diffraction dissociation ? We believe, however, consistently with the Good-Walker interpretation, that the extreme broadness of the proton-proton eigenamplitude spectrum gives us an important clue suggesting that the proton has a very rich internal structure. We are now actively studying the above and related problems.

5. EIKONAL PICTURE

It was stressed by Blankenbecler [10] that the effect of rising inelastic diffraction on the total cross-section is destructive, i.e., if the non-diffractive cross-section, in the absence of diffraction, stays constant but new diffractive channels open up, the total cross-section decreases instead of increasing. This result was derived for a large class of Feynman diagrams. It holds also in the multi-channel eikonal approach and in the Gribov Reggeon calculus approach.

As we have seen, the energy dependence of σ_{diff} is not very well known. We can, however, be rather sure that σ_{diff} is not decreasing by many millibarns over the FNAL-ISR range. Consequently, the rise of the total cross-section must originate from the non-diffractive dynamics (the "bare" Pomeron intercept is above one ?). A possible increase of σ_{diff} would just emphasize this point.

The negative rescattering effects caused by the inelastic diffractive channels have quite a spectacular effect on the eikonal analysis of elastic scattering data. As is well known, the Chou-Yang model [11] (where the eikonal is determined by the overlap of two matter distributions whose shape is given by the electromagnetic form factors) has been quite successful in describing the t dependence of elastic scattering [12]. However, it turns out that when the influence of inelastic diffractive channels is properly taken into account in the analysis, the resulting picture is quite different from that of Chou and Yang.

To investigate this question, we have carried out a series of numerical calculations in the multichannel eikonal framework. Since not much is known about the off-diagonal eikonal elements $\Omega_{ik}(b)$, $(i \neq k)$, the results vary considerably. They have, however, one common feature : in all cases the elastic element $\Omega_{11}(b)$ deviates strongly from the Chou-Yang eikonal at moderate b and agrees with it only at large b. We illustrate this point in the two-channel approximation, where the diffractive t matrix and the eikonal are 2×2 matrices with all the inelastic diffraction included as a single off-diagonal element. Such an approximation is obviously very simplistic and the following results should be regarded as an illustration only. We make the simple assumption that the impact parameter dependence of all the eikonal elements is the same. We can then find the common b dependence of the eikonal elements from experimental data on elastic scattering, adjusting the remaining parameters to satisfy the experimental lower limits for integrated diffractive cross-section. A typical result is sketched in Fig. 5. We see that a large excess above the Chou-Yang curve at small b values appears in the eikonal.

The above result suggests that the matter distribution of the proton is different from the charge distribution. That this should be so, is actually not very surprising. The electromagnetic form factor describes the distribution of charged constituents of the proton and some data (e.g., from deep inelastic electroproduction [13]) show the importance of neutral constituents carrying a large part of proton momentum. Our analysis suggests that this "neutral core" is very important in the strong interaction processes. This agrees nicely with some parton-gluon schemes of particle production [14]. Unfortunately, we are unable to determine accurately the shape of the neutral contribution since the possible differences in the b dependences of the elastic and inelastic eikonal elements (expected, e.g., from the spin structure) may affect significantly the details of our results.

To conclude this Section, we note that a detailed study and further development of the multi-channel eikonal approach would be very interesting. We have not yet proceeded very far on this line of study but it is obvious that many new effects are to be expected. For example, one may have all the eikonal elements increasing indefinitely but still get an arbitrarily small elastic amplitude. Thus the saturation of the black disc limit is by no means a necessary result following from an increasing "bare" amplitude, as is the case for the standard "scalar" analysis. This result, known already to several authors, should be kept in mind in the following discussion of the asymptotic region.

6. ASYMPTOTIC PICTURE

The impact parameter representation has been widely used to analyze the high energy behaviour of elastic scattering and to speculate about asymptotic behaviour. In particular, Cheng and Wu [15] have predicted that the amplitude should saturate the black disc limit, whereas phenomenological analyses of data have led other authors to the "geometrical scaling" picture [16] where the energy dependence appears only as a change in the impact parameter scale. We would now like to speculate what kind of asymptotic behaviour may be expected from an extrapolation of the existing data as analyzed in our approach.

First, let us repeat once more that the Pumplin bound (6) allows the elastic amplitude to saturate the black disc limit only if the inelastic diffraction is negligible. In fact, this was one of the conclusions of the Cheng-Wu model [17]. However, as we have seen from the compilation of Fig. 3, there is no experimental evidence whatsoever for σ_{diff} decreasing relative

to σ_{el}. Even in the energy range where other "asymptotic phenomena" (as rising σ_{tot} and σ_{el}) are seen, the ratio $\sigma_{diff}/\sigma_{el}$ seems to increase, or at least to stay constant. Thus, the simplest extrapolation of data compatible with rising cross-sections and with the Pumplin bound gives the "grey disc limit" - the hadrons stay asymptotically semi-transparent. If the approximate equality $\sigma_{diff} \simeq \sigma_{el}$ is assumed to hold asymptotically, the maximal average opacity allowed by unitarity is about $\frac{1}{2}$. This value can be exceeded for small impact parameters, for which the spin structure discriminates inelastic diffraction (remember that inelastic diffraction does not conserve s channel helicity and that an amplitude corresponding to a helicity flip of n units vanishes at small b as b^n). Thus the effective unitarity limit may be of the shape sketched in Fig. 6. The detailed shape of the amplitude obviously cannot be predicted from our oversimplified approach. We want to stress here, however, that including inelastic diffraction, we find the effective unitarity limit to be nearly saturated by data for small b. This explains the apparent energy independence of the elastic profile in this region and may account for the applicability of the approximate geometrical scaling.

7. CONCLUSIONS

As we have seen, the unified description of elastic and inelastic diffractive channels allows one to modify many ideas about the diffractive scattering. The global inelastic contribution (when evaluated in the proper scale) appears to be very large, suggesting rather unexpected behaviour of the spectrum of eigenamplitudes to which the physical particles couple. Our results suggest important deviations from the standard eikonal analysis and from the asymptotic predictions derived in the models neglecting inelastic diffraction. There are also many other effects which we have not discussed here. Thus, for example, average multiplicity and the multiplicity distributions are affected, which may remove some discrepancies between the Cheng-Wu model and data.

To conclude, we believe that, although our present approach is very oversimplified and any of our numerical results should be taken cautiously, our analysis shows the usefulness of the unified treatment of elastic and inelastic diffraction. It should be pursued further and, subsequently, applied in all the phenomenology. The resulting modifications of models and the new theoretical insights to be gained will certainly constitute a step forward towards better understanding of strong interactions.

REFERENCES

1) L. Caneschi, P. Grassberger, H.I. Miettinen and F. Henyey, Phys.Letters 56B, 359 (1975).

2) K. Fiałkowski and H.I. Miettinen, Semi-transparent hadrons from multi-channel absorption effects, CERN preprint TH.2057 (1975) - to be published.

3) J. Pumplin, Phys.Rev. D8, 2899 (1973).

4) P. Pirilä, P.V. Ruuskanen and H.I. Miettinen - in preparation.

5) E.g., G.L. Kane, Acta Phys.Polon. B3, 845 (1972).
For more recent quantitative data analyses, see, for example :
N. Sakai and J.N.J. White, Nuclear Phys. B59, 511 (1973); and
S. Humble, Nuclear Phys. B86, 285 (1975).

6) M.L. Good and W.D. Walker, Phys.Rev. 126, 1857 (1960).
See also :
E.L. Feinberg and I. Pomeranchuk, Suppl.Nuovo Cimento 3, 652 (1956).

7) The experimental estimates for inelastic diffraction are from :
a) S.J. Barish et al., Phys.Rev.Letters 31, 1080 (1973); Phys.Rev. D9, 2689 (1974).
b) J. Benecke et al., Nuclear Phys. B76, 24 (1974).
c) C.H. Bromberg et al., Michigan preprint UMBC 72-14 (1972).
d) J.W. Chapman et al., Phys.Rev.Letters 32, 257 (1974).
e) F.T. Dao et al., Phys.Letters 45B, 399, 402 (1973).
f) R.D. Schamberger et al., Phys.Rev.Letters 34, 1121 (1975).
g) J. Whitmore, Phys.Reports 10C, 273 (1974).

8) D.P. Roy and R.G. Roberts, Nuclear Phys. B77, 240 (1974).

9) See, for example, A. Białas, W. Czyż and A. Kotanski, Ann.Phys. 73, 439 (1972);
J. Pumplin, Phys.Rev. D7, 795 (1973).

10) R. Blankenbecler, Phys.Rev.Letters 31, 964 (1973).

11) T.T. Chou and C.N. Yang, Phys.Rev. 170, 1591 (1968).

12) Among many successful applications, see, e.g.,
L. Durand III and R. Lipes, Phys.Rev.Letters 20, 637 (1968);
B. Carreras and J.N.J. White, Nuclear Phys. B32, 319 (1971);
M. Kac, Nuclear Phys. B62, 402 (1973).

13) G. Miller et al., Phys.Rev. D5, 528 (1972).

14) L. Van Hove and S. Pokorski, Nuclear Phys. B86, 243 (1975).

15) H. Cheng and T.T. Wu, Phys.Rev.Letters 24, 1456 (1970).

16) J. Dias de Deus, Nuclear Phys. B59, 231 (1973).
For a discussion of more recent data in this model, see, e.g. :
V. Barger, Rapporteur's talk at the XVII International Conference on High Energy Physics, London (1974).

17) J.K. Walker, Proceedings of the 8th Rencontres de Moriond, p.159 (1973).

* * * * *
* * * * *
* * * *
*

FIGURE CAPTIONS

Figure 1 : Impact parameter distributions for pp scattering at $s = 53$ GeV [1]. Elastic and total cross-sections are shown as dashed and dash-dotted lines, respectively. The solid line is a resulting bound for $\sigma_{diff}(b)$.

Figure 2 : Schematical illustration of eigenamplitude spectrum. Probability density for a proton-proton state being coupled to eigenstates of given opacity t_k is plotted versus t_k.

Figure 3 : A compilation of $\sigma_{diff}/\sigma_{el}$ estimates for pp scattering. Crosses, circles, dots, squares, sexagones, down- and up-edged triangles represent the data of Refs. 7a)-7g), respectively. The curve results from the fit of Ref. 8).

Figure 4 : Various possible probability distributions describing the decomposition of pp state into diffractive eigenstates for three values of b. Resulting integrated diffractive cross-section σ_{diff} is presented in the last column for each distribution.

Figure 5 : Dashed line is an example of eikonal calculated assumed two-channel approximation and a common b dependence of all the eikonal matrix elements. Corresponding σ_{diff} is about 6 mb. Chou-Yang fit calculated from the dipole form factor (12) is shown as a solid line.

Figure 6 : Suggested asymptotic limit (shaded line) as compared with the black disc limit and energy dependence of experimental shape of elastic profile [4].

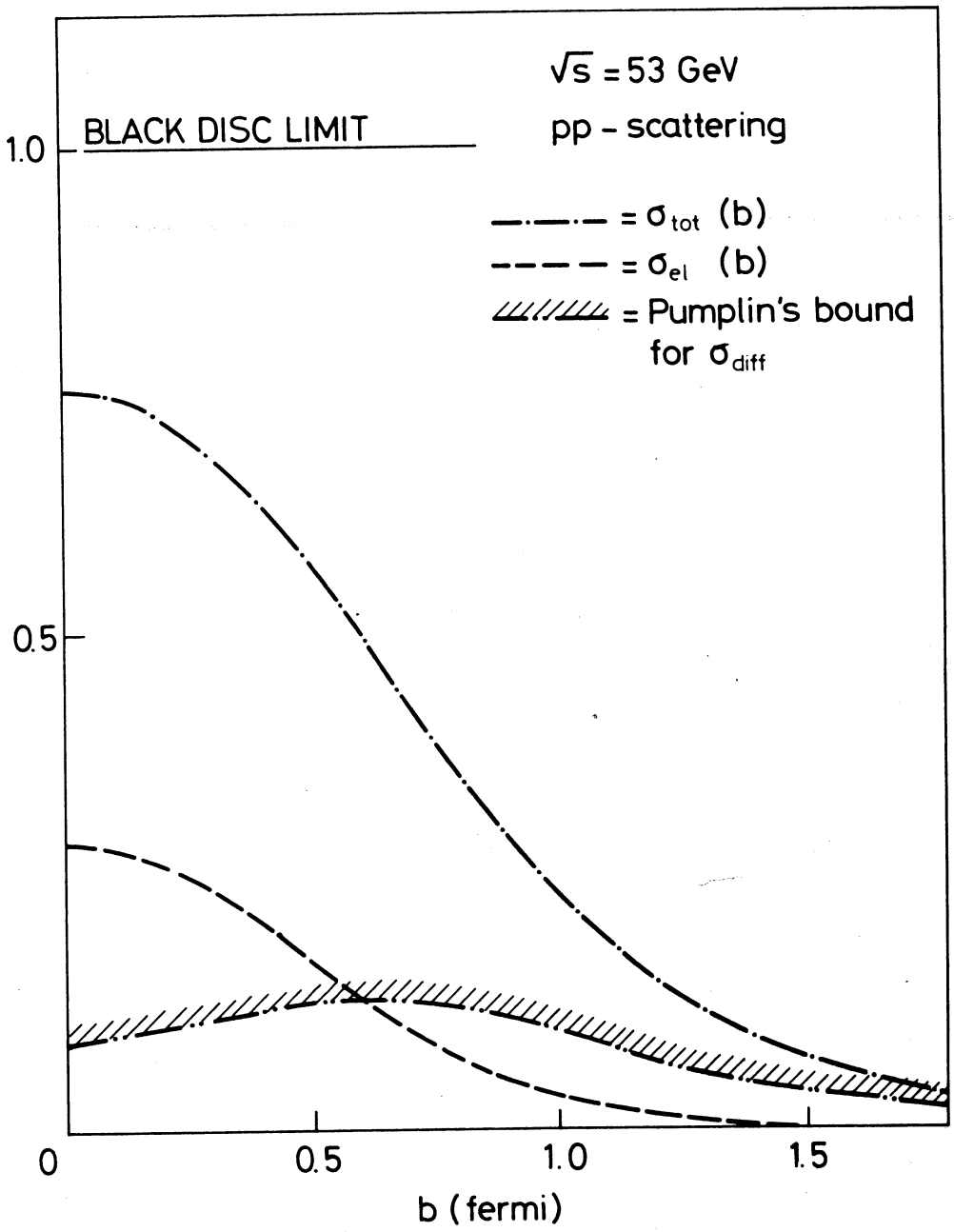
√s = 53 GeV
pp - scattering
BLACK DISC LIMIT
1.0
= σtot (b)
= σel (b)
= Pumplin's bound for σdiff
0.5
0
0.5
1.0
1.5
b (fermi)

Fig. 1

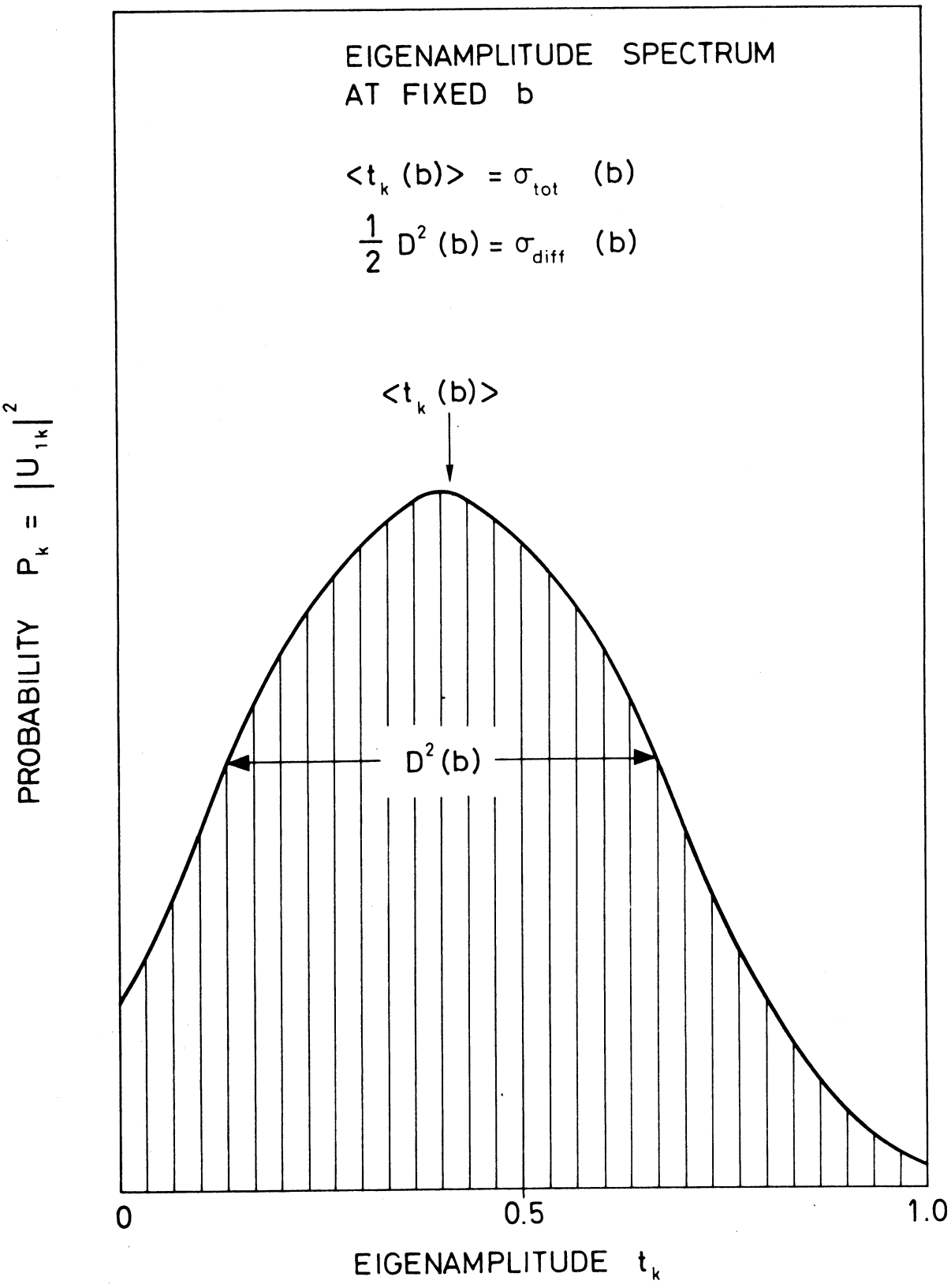
EIGENAMPLITUDE SPECTRUM
AT FIXED b
$\langle t_k(b) \rangle = \sigma_{tot}(b)$
$\frac{1}{2} D^2(b) = \sigma_{diff}(b)$
$\langle t_k(b) \rangle$
$D^2(b)$
PROBABILITY $P_k = |U_{1k}|^2$
0
0.5
1.0
EIGENAMPLITUDE t_k

Fig. 2

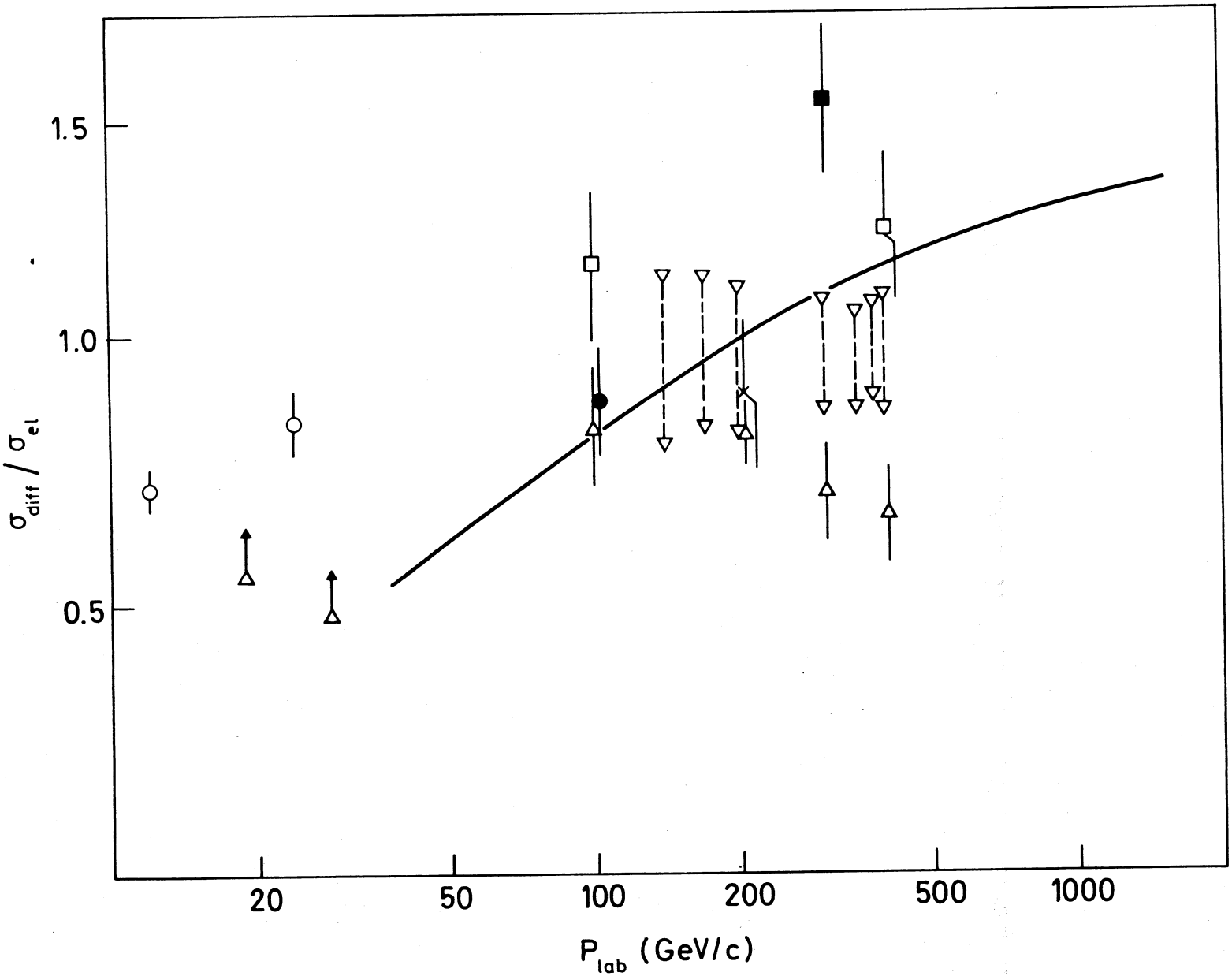

Fig. 3

SPECTRUM	$b \approx 0$ $\langle t \rangle = 0.75$	$b \approx 0.6\,f$ $\langle b \rangle = 0.5$	$b \approx 1.0\,f$ $\langle b \rangle = 0.25$	σ_{diff} [mb]
TRIANGLE	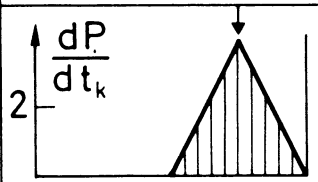	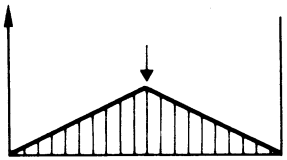	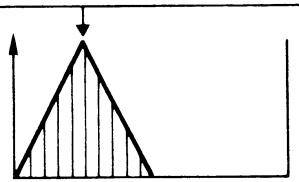	~1.0
RECTANGLE	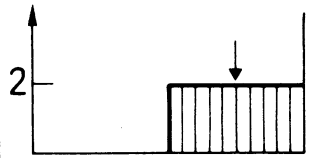	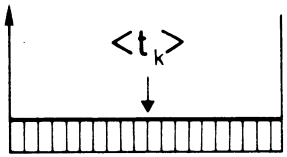	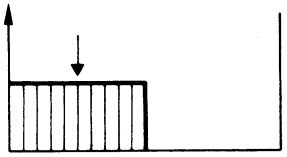	~1.9
LINEAR	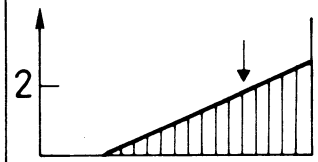	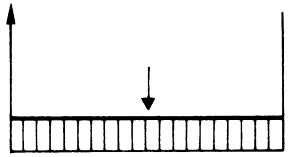	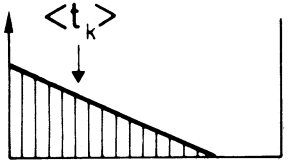	~2.3
DOUBLE LINEAR	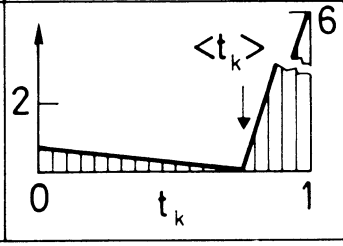	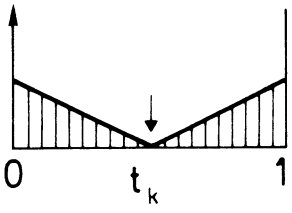	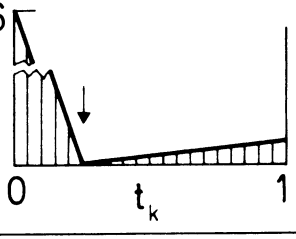	~6.3

Fig. 4

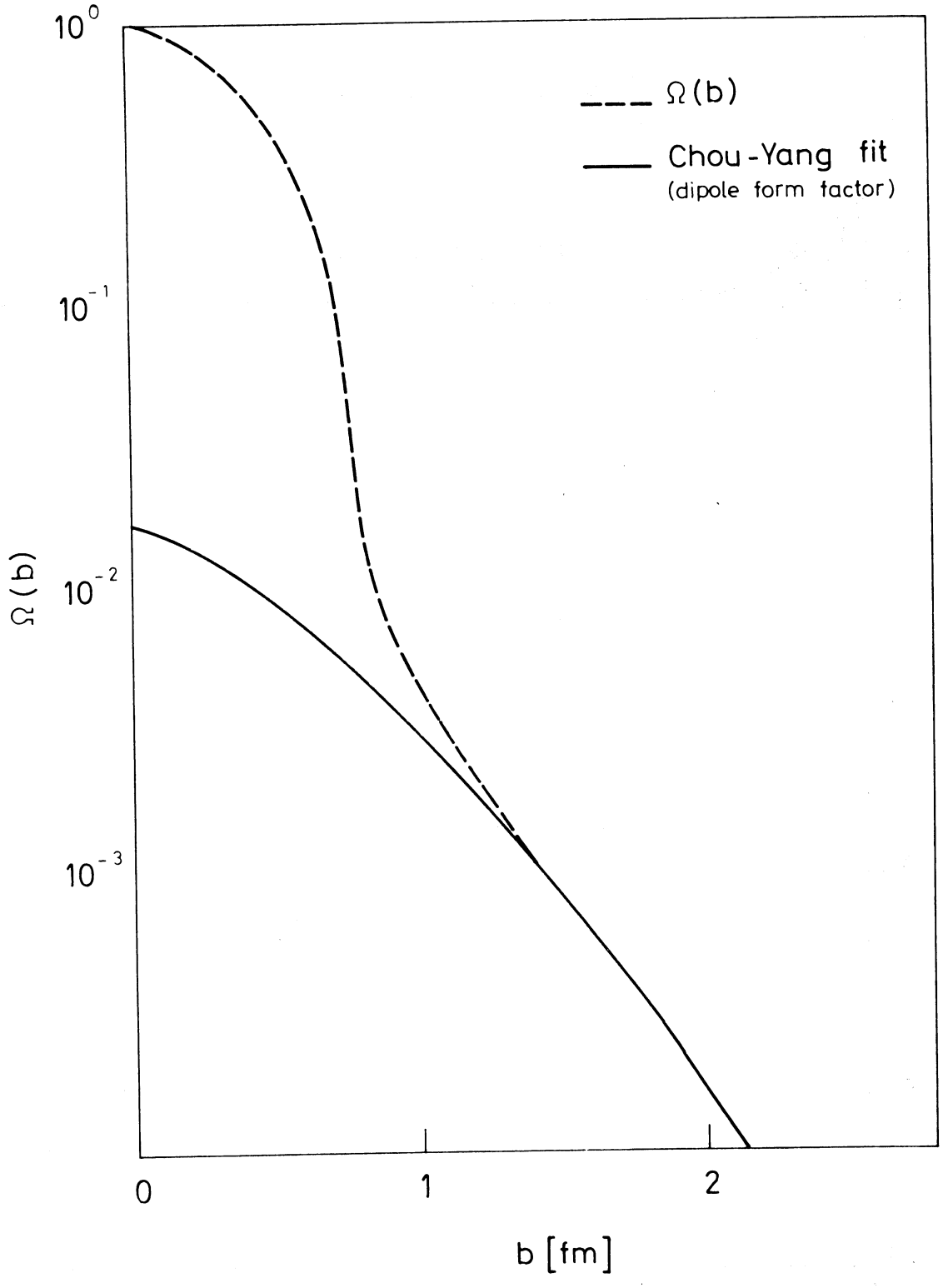

Fig. 5

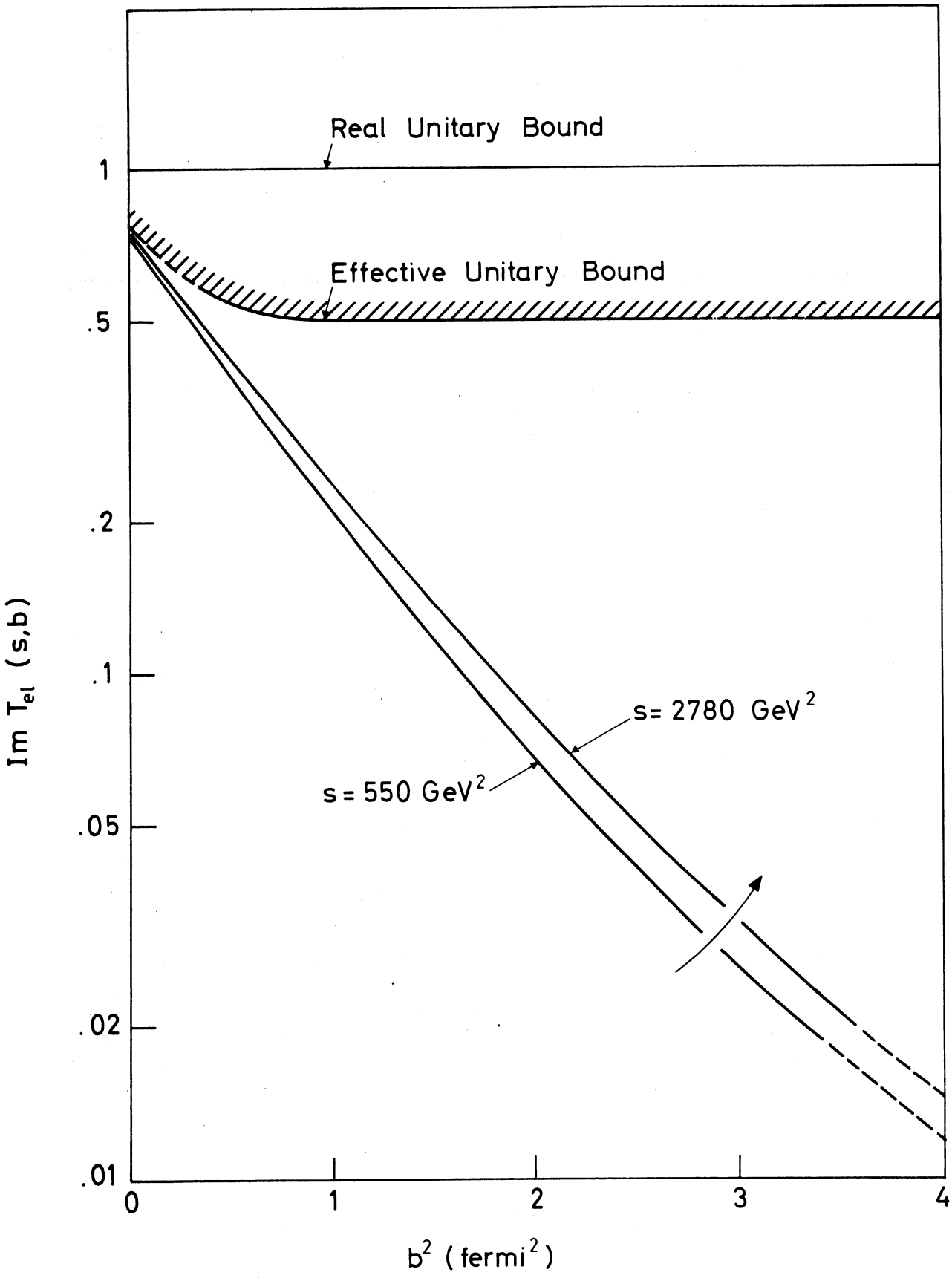
Real Unitary Bound
Effective Unitary Bound
s= 2780 GeV 2
s = 550 GeV 2
1
.5
.2
.1
.05
.02
.01
0
1
2
3
4
Im T el (s,b)
b 2 (fermi 2)

Fig. 6